Video Article

Data Processing Methods for 3D Seismic Imaging of Subsurface Volcanoes: Applications to the Tarim Flood Basalt

Lei Wang[1], Wei Tian[2], Yongmin Shi[2]

[1]College of Engineering, Peking University

[2]School of Earth and Space Sciences, Peking University

Correspondence to: Wei Tian at davidtian@pku.edu.cn

URL: https://www.jove.com/video/55930
DOI: doi:10.3791/55930

Keywords: Bioengineering, Issue 126, Reflection seismology, 3-D seismic interpretation, well logging, synthetic seismogram, surface probes, opacity rendering, time slice, subsurface volcano, Tarim flood basalt

Date Published: 8/7/2017

Citation: Wang, L., Tian, W., Shi, Y. Data Processing Methods for 3D Seismic Imaging of Subsurface Volcanoes: Applications to the Tarim Flood Basalt. *J. Vis. Exp.* (126), e55930, doi:10.3791/55930 (2017).

Abstract

The morphology and structure of plumbing systems can provide key information on the eruption rate and style of basalt lava fields. The most powerful way to study subsurface geo-bodies is to use industrial 3D reflection seismological imaging. However, strategies to image subsurface volcanoes are very different from that of oil and gas reservoirs. In this study, we process seismic data cubes from the Northern Tarim Basin, China, to illustrate how to visualize sills through opacity rendering techniques and how to image the conduits by time-slicing. In the first case, we isolated probes by the seismic horizons marking the contacts between sills and encasing strata, applying opacity rendering techniques to extract sills from the seismic cube. The resulting detailed sill morphology shows that the flow direction is from the dome center to the rim. In the second seismic cube, we use time-slices to image the conduits, which corresponds to marked discontinuities within the encasing rocks. A set of time-slices obtained at different depths show that the Tarim flood basalts erupted from central volcanoes, fed by separate pipe-like conduits.

Video Link

The video component of this article can be found at https://www.jove.com/video/55930/

Introduction

The aim of most of the industrial seismic imaging projects in sedimentary basins is to explore for hydrocarbon reservoirs. In recent years, hydrocarbon exploration has expanded to basins containing large amounts of igneous rocks because many of the volcanogenic basins have considerable oil and gas reservoirs. However, because of the interface of igneous rocks in the volcanogenic basins, seismic data processing presents a series of challenges induced by various intrusions, such as reduced energy transmission, intrinsic attenuation, interference effects, refraction and scattering[1]. Therefore, oil field companies are focusing their efforts on reducing such a "negative impact" on seismic imaging[2,3,4].

Igneous bodies within sedimentary basins are easily identified by two dimensional or 3D seismic reflection imaging due to the large acoustic impedance contrast with the encasing rocks[1,5,6]. This method can provide spectacular images of both vertical and horizontal structures of the volcanic plumbing systems[7,8,9,10,11,12,13]. However, the strategies of imaging subsurface volcanos are very different from that of oil and gas explorations[8,14,15]. This has limited the use of industrial seismic data in studies of subsurface volcanoes, apart from a few successful cases[10,15,16]. In this paper, we report detailed procedures of seismic data processing, which are customized for interpretation of subsurface volcanoes. We process two seismic cubes, TZ47 and YM2 (**Figure 1**), to show how to visualize the buried igneous bodies in the Tarim flood basalt[17].

Protocol

NOTE: The data processing procedures include: synthetic seismogram calculation, synthetic-real seismic trace correlation, and geo-body extraction. Below are the step-by-step details of each procedure.

1. Calculation of Synthetic Seismogram

1. Calculate the acoustic impedance at each interval of the down-well logging curve.
   NOTE: Acoustic impedance is the product of 'seismic wave velocities' and 'density' (ρ*v)). The data are often averaged to sampling intervals larger than 1 ft, in order to reduce the computation time and aliasing.
2. Calculate the reflection coefficients (R_0) at each interface by using the acoustic impedance calculation:

$$R_0 = \frac{\rho_2 v_2 - \rho_1 v_1}{\rho_2 v_2 + \rho_1 v_1}$$

where v_1 and v_2 are the averaged velocities of the layers below and above the interface, respectively; ρ_1 and ρ_2 are the corresponding averaged densities.

1. If the well does not intersect the igneous bodies, use nearby wells that have intersected the target rocks to obtain the parameters (velocity, density, *etc.*).

3. Chose a wavelet that has an amplitude and phase spectrum similar to that of the nearby seismic data.
4. Convolve the synthetic wavelet with the reflection series for the entire well survey and generate a synthetic seismic trace. The final simulated seismic trace $T(t)$ can be described by the convolutional model as below:
$$T(t) = R_0(t) \times w(t) + n(t)$$
where $R_0(t)$ is the reflection coefficient, $w(t)$ is the wavelet and $n(t)$ is the noise.
5. If the frequency of the seismic data has large variations throughout the whole well, re-compute the synthetic seismic trace using a wavelet with a different phase and a dominant frequency at different depth intervals.
    1. Repeat the process if the match between the synthetic trace and the seismic data is not satisfactory.

6. Perform the calculation with the provided software (*e.g.*, Petrel E&P Software Platform).
    1. Start the software. Select **File** | **Open Project** | and then select the demo research project **tlm** (users can select their own desired projects). The project should contain well data, wired log, well tops, seismic cube, and interpretation surface in the research area.
    2. Click on **Home** | **Windows** | **2D Windows** | **3D Windows** to open two display windows to show the data sets according to user's preference.
    3. In the "Wells Tree of Input Pane", right click the desired well. Open the **Settings** window of the well and select the **Time** tab to create a new time log. Select **Velocity Function**, then select **DT** data in the new time log. Click the **OK** button to close settings window. A new one-way time log is automatically created and will be shown in the "Wells Tree of Input Pane".
    NOTE: A one-way time log is a time-depth relationship of this well. Wired log domains can be transformed to time domains and be shown in the time domain window.
    4. Activate an existing **3D Window** by clicking the displayed window. If there is no **3D Window** displayed, create a new **3D Window** by clicking **Home** | **Windows** | **3D Windows**. Select **TWT** in the toolbar of the 3D Window to show the 3D Window in time domain.
    5. Select representative wired logs (such as 'GR', 'DT', or 'RT') in the **Wells Tree** to show them in the 3D Window; at the same time, select the seismic profile in the 'seismic' tree of the 'input' pane to show them in the same 3D Window.
    6. Use the **Manipulate Plane** tool in the toolbar of the 3D Window to adjust the location of the profile to intersect the well; the user will see that the wired log has been transformed to the time domain and displayed with the seismic profile in the same 3D window.
    7. Click **Seismic Interpretation** | **Seismic Well Tie** | **Seismic Well Tie Process**. Choose **Integrated Seismic Well Tie** in the type of study row, and add desired well in the Well row. Choose calibrated one-way time log as time-depth relationship in the TDR row of the input tab, choose seismic cube in the seismic row. Choose any log in the RC calculation method.
    8. Click **Launch Wavelet Toolbox** to create a Ricker wavelet to apply in this process. Click **OK** and a new well section window and synthetic seismogram display will be created.

2. Correlate the Synthetic Traces with the Real Seismic Reflectors

1. Use an automated correlation application, like **Seismic Well Tie** in the platform, to adapt the resulting synthetic trace to the vertical scale of the seismic section.
2. Adjust the synthetic seismogram to increase the overlapping of high amplitude reflectors of the synthetic trace and real trace.
3. Adjust the synthetic seismogram and the real trace repeatedly. When the overlapping trace reaches the maximum, the interpreter has reached the "best fits" between the obtained synthetic seismogram and real traces.
    1. Repeat the process until the correlations reach the desired level.

4. Perform the correlation with the provided software.
    1. Activate the window created in step 1.6.3, which is the one-way time log automatically created from the acoustic log.
    NOTE: This automatically created 'one-way time log' is not perfectly correlated with the real seismic reflectors. The users should calibrate the correlations between the one-way time log and the real seismic reflectors.
    2. To calibrate their correlations, choose a continual and representative reflector that is intersected by the well. Then manually adjust the depth of the well log. For example, to adjust the depth of the DT log, right click the **One-Way Time Log** in well tree | select the **Calculator** tool | then add a small time increment (for example, 10 ms) by typing 'DT=DT+10' in the input dialog of the Calculator tool.
    3. If the '10 ms' increment is too large or too small, change the increment to another time (can be negative value) in the 'calculator' tool. Check the correlation between the well log and the selected seismic horizon repeatedly and then adjust the time increment repeatedly, until the correlation is perfectly calibrated.

3. Extraction of Basaltic Sills

1. Pick 2 high-amplitude reflectors encasing the target sills.
NOTE: Most intrusions are expressed in seismic data as tuned reflection packages, whereby the reflections from the upper and lower intrusion contacts cannot be distinguished. Tuning occurs when the vertical intrusion thickness is between λ/4 and λ/8 (λ is seismic wavelength)[19]. Therefore, sills are shown as a set of strong reflections in the seismic section, and their apparent thickness is false.
2. Extract probes between the horizons corresponding to the two high-amplitude reflectors.
NOTE: There are different tools based on the rendering technique that can help the interpreters better visualize the targets, such as "box probes", "surfaces probes" and "well probes". However, for identification of contacts between the sills and encasing strata, the best tool is "surface probe". ("Surface probe, *etc.*" are terms in 'Petrel' software. The software users should be familiar with these terms).

3. Remove the areas surrounding the geological objects of interest by changing the Voxel connectivity opacity threshold value. Set the default threshold value to 20%. The visualization method of "opacity rendering" is used here to display the result of the extraction of basaltic sills (**Figure 2C**).
   NOTE: There are high amplitude reflections along the surface between igneous rock and sedimentary rock because of their significant difference in acoustic impedance. Make the low amplitude parts transparent to highlight the shape of the igneous bodies.
4. As the value for isolation can be higher than 20 - 30%, change the value with small increments to make sure all important igneous bodies are not lost; the larger the value, the higher the risk of losing the volume of the real igneous bodies.
5. Perform the operation with the provided software.
   1. Click the **Seismic Interpretation** pane, click **Insert a Horizon Probe**. A probe will be added in the geobody interpretation probes tree of input pane. Double click the added horizon probe and a pop-up window will appear.
   2. Click the **Horizons** tab in the pop-up window and choose two seismic surfaces that isolate the zone of sills. Click **OK** to apply the operation.
   3. Check the newly added probe in the geobody interpretation probes tree shown in the input pane. A seismic cube will then appear in the 3D window.
   4. Double click the probe and choose the **Opacity** tab. A histogram of seismic amplitude will be shown in the tab. Use the left mouse button to draw a line in the histogram to control the opacity of the seismic cube. The low amplitude parts of the tube should be invisible and the high amplitude parts will be left.
   5. Adjust the histogram repeatedly until the desired shape of the interested geobody is achieved.

4. Extraction of the Feeding Conduits

1. Choose continuous and high energy reflection horizons at different depths beneath the surface lava flow.
2. Do time slicing along the selected horizons, to find out discontinuities corresponding to the vertical conduits.
3. Adjust the Two-Way Time (TWT) repeatedly, to achieve the best imaging of the discontinuities of the conduits.
   NOTE: Seismic data cannot image vertical structures well, so better images from amplitude volumes and variance volumes are chosen by comparing clearness at different travel times.
4. Try different slicing techniques, and then choose which can better image the discontinuities.
   NOTE: Different tools can be used here, such as variance body slicing. Its theoretical basis is the similarity between each seismic section and adjacent seismic traces in the seismic data. Another tool, the variance cube, is a new data body processed by the conventional seismic data, which is helpful for the identification of changes in the structure and lithology, plane combination of the fault, *etc.*[20]
5. Plot the slices at different travel times or depths into a 3D space.
6. Perform the operation with the provided software.
   1. Double click **Volume Attributes** in the geophysics tree of the processes pane. Check **Structural Methods** in the category column and **Variance** in the attribute column. Select the seismic cube to input box and adjust the other parameter in the parameter tab. For better reading performance, check the box in the realize column. A variance cube is created in the seismic tree of the input pane.
   2. Right click the variance cube and click **Insert Time Slice Intersection** to show more horizontal intersections in the 3D window. Use the **Manipulate Plane** tool in the toolbar of the 3D window to adjust the location of the slices to optimize the display of conduits.
   3. Right click the seismic amplitude cube and click **Insert Time Slice Intersection** to show more horizontal intersections in 3D window. Do the same operation as step 4.6.2 to adjust the location of the slices to optimize the display of conduits.

Representative Results

We demonstrate the usefulness of the techniques described above by applying them to 2 types of igneous bodies, horizontal sills and vertical volcanic conduits. Extraction of the sills is conducted by using the opaque rendering technique, and interpretation of the volcanic conduit is performed by using slicing technique.

Extraction of sills

Industrial drilling wells have intersected many sills in the Yingmai-2 area from the Northern Tarim Basin[17], but the 3D distribution of the sills remains unclear. In order to interpret the sills, we process 3D seismic data from a seismic cube in this area. Firstly, we identify the horizons related to the presence of the sills in the seismic cube by correlating the synthetic seismograms with the seismic cross-sections (**Figure 2A**). Then we insert surface probes (**Figure 2B**) into the horizons to constrain the lateral extent of the sills. Finally, we use opacity rendering to extract the geo-bodies of sills (**Figure 2C**) from the seismic cube. We find that the sills turn to separated lava lobes at the distal end, which indicates that the flow direction is from the dome center to the rim of the dome (**Figure 2C**).

Interpretation of volcanic conduit

Following the steps detailed in section 4, we obtain six time slices at different depths in the original seismic cube (**Figure 3A**). Variance body time slices are also shown (**Figure 3B**). We choose different slicing depths for the variance body time slices because the best resolution of this method is achieved at depths different from that in the original seismic cube. It is clear that the conduits can be imaged by the time slicing technique.

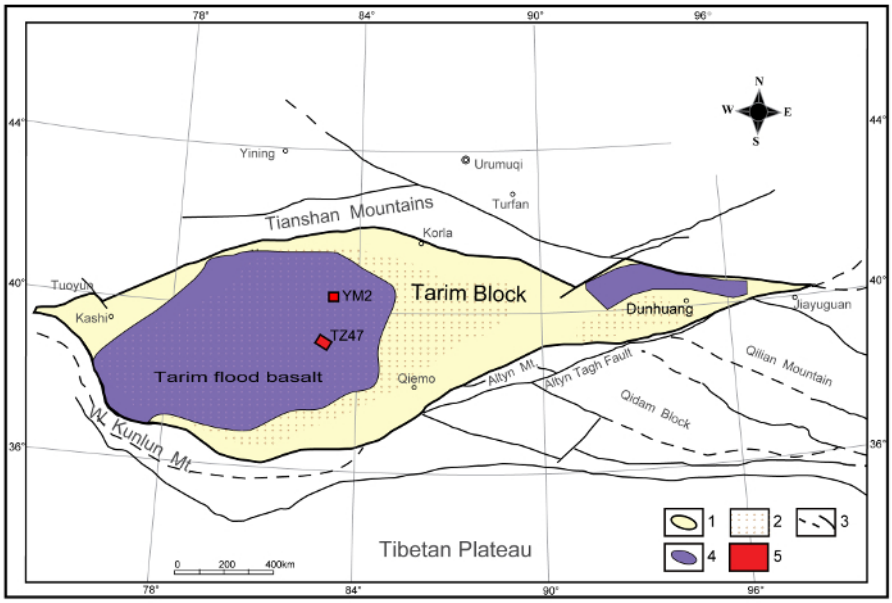

Figure 1: Sketch Geological Map of the Tarim Continental Flood Basalt[18] and the Location of the Seismic Cubes.
1. Tarim block; 2. Desert; 3. Major fault; 4. Flood basalt; 5. Seismic cubes. Please click here to view a larger version of this figure.

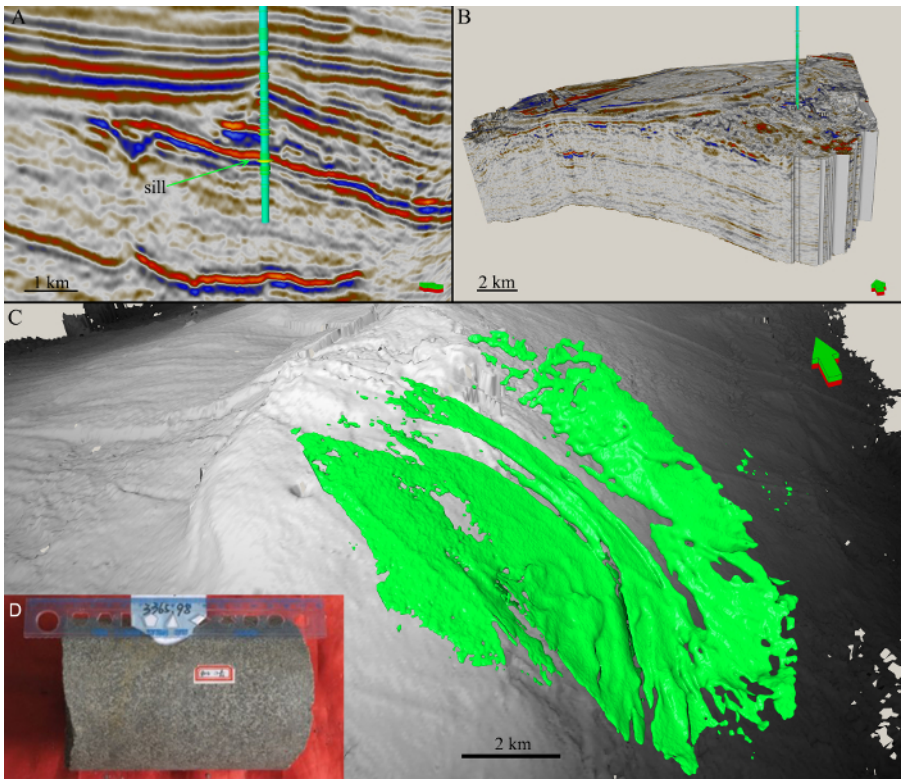

Figure 2: Procedures of Extracting the Geo-bodies of Basaltic Sills Encased in Sedimentary Strata.
A. Correlation between the synthetic seismogram (green bars around the drilling well) and the seismic cross section; **B**. Surface probes along the horizon of sills; **C**. The extracted geo-bodies of the sills, which is located above the dome center (colored with gray scale); **D**. A typical dolerite drilling core sample from the TZ47 area. Please click here to view a larger version of this figure.

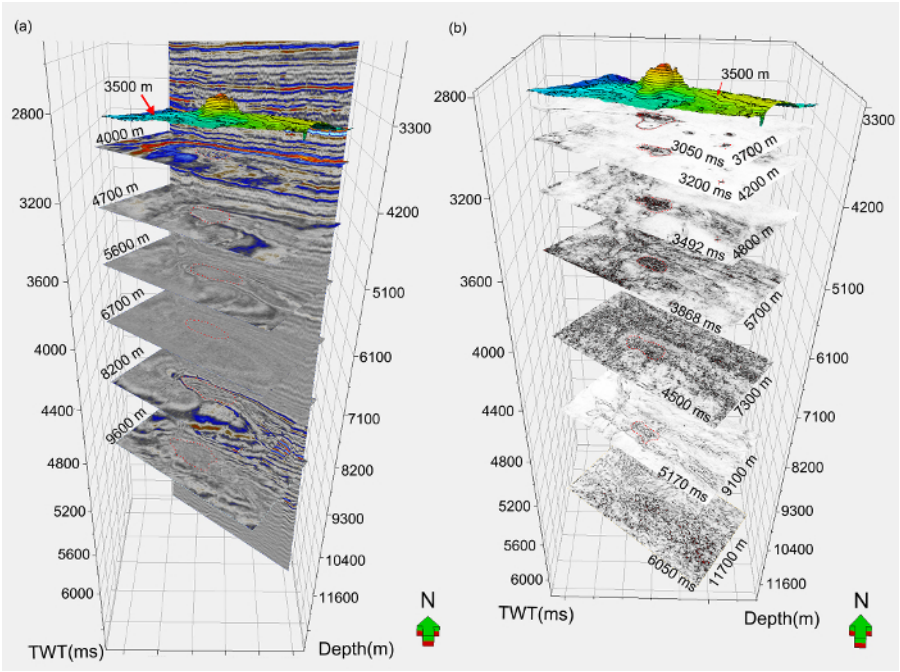

Figure 3: Three-dimensional Structure of the Conduits.
Imaged by time slice of the original seismic cube (**A**) and of the re-computed coherent body seismic cube (**B**). Please click here to view a larger version of this figure.

Discussion

Here we demonstrate 2 methods for illustrating the morphology and structure of the plumbing system of buried basaltic volcanoes; one is opacity rendering, the other is time slicing.

The opacity rendering method is suitable for geo-bodies that have continuous and near horizontal interfaces with the encasing strata. With this method, one can extract the 3D morphology of magma lobes. Normally, flow directions should be along the long axis of the magma lobes. It is also important that the surface horizons have high reflection coefficients (R_0). If the R_0 is too low at the interface, interpreters will not be able to insert surface probes to the target horizons. For example, sonic velocity of basaltic sills is around 5500 m/s, and carbonates have similar velocity of 6,000 m/s[12]. Thus, the reflection coefficient at the sill-carbonate contacts would be too low to be identified by surface probes. When using this technique, precise knowledge of the velocities of the target rocks is required. If the velocity data are not available or not properly estimated, application of this method to seismic cubes will be highly limited.

The time slicing method can apply to geo-bodies that have no continuous and horizontal surfaces. When the igneous intrusions have sonic velocities very different from the encasing rock (in most cases, higher than the encasing rock), interpreters can use the time slicing technique to image the boundaries between the intrusions and the surrounding rocks. If the wall rock have similar sonic velocities, it is also very difficult to identify the igneous intrusions from the country rocks.

Disclosures

The authors have nothing to disclose.

Acknowledgements

The authors acknowledge the financial support of NSFC to WT (grant no. 41272368) and QKX (grant no. 41630205).

References

1. Smallwood, J. R., & Maresh, J. The properties, morphology and distribution of igneous sills: modelling, borehole data and 3D seismic from the Faroe-Shetland area. *Geol. Soc. London Spec. Publ.* **197** (1), 271-306 (2002).
2. Millett, J. M., Hole, M. J., Jolley, D. W., Schofield, N., & Campbell, E. Frontier exploration and the North Atlantic Igneous Province: new insights from a 2.6 km offshore volcanic sequence in the NE Faroe-Shetland Basin. *J. Geol. Soc.* **173** (2), 320-336 (2016).
3. Lee, G. H., Kwon, Y. I., Yoon, C. S., Kim, H. J., & Yoo, H. S. Igneous complexes in the eastern Northern South Yellow Sea Basin and their implications for hydrocarbon systems. *Mar. Pet. Geol.* **23** (6), 631-645 (2006).
4. Rateau, R., Schofield, N., & Smith, M. The potential role of igneous intrusions on hydrocarbon migration, West of Shetland. *Pet. Geosci.* **19** (3), 259-272 (2013).

5. Magee, C. *et al.* Lateral magma flow in mafic sill complexes. *Geosphere.* **12** (3), 809-841 (2016).
6. Magee, C., Jackson, C. A. L., & Schofield, N. Diachronous sub-volcanic intrusion along deep-water margins: insights from the Irish Rockall Basin. *Basin Res.* **26** (1), 85-105 (2014).
7. Symonds, P., Planke, S., Frey, O., & Skogseid, J. Volcanic evolution of the Western Australian continental margin and its implications for basin development. *The sedimentary basins of Western Australia.* **2** 33-54 (1998).
8. Thomson, K., & Hutton, D. Geometry and growth of sill complexes: insights using 3D seismic from the North Rockall Trough. *BVol.* **66** (4), 364-375 (2004).
9. Planke, S., Rasmussen, T., Rey, S., & Myklebust, R. in *Petroleum Geology: North-West Europe and Global Perspectives-Proceedings of the 6th Petroleum Geology Conference.* Vol. 6 (eds A. G. DORE´ & B. A. VINING) 833-844 Geological Society, London (2005).
10. Magee, C., Hunt Stewart, E., & Jackson, C. A. L. Volcano growth mechanisms and the role of sub-volcanic intrusions: Insights from 2D seismic reflection data. *Earth Planet. Sci. Lett.* **373** 41-53 (2013).
11. Schofield, N. J., Brown, D. J., Magee, C., & Stevenson, C. T. Sill morphology and comparison of brittle and non-brittle emplacement mechanisms. *J. Geol. Soc.* **169** (2), 127-141 (2012).
12. Wang, L., Tian, W., Shi, Y. M., & Guan, P. Volcanic structure of the Tarim flood basalt revealed through 3-D seismological imaging. *Sci. Bull.* **60** (16), 1448-1456 (2015).
13. Sun, Q. *et al.* Neogene igneous intrusions in the northern South China Sea: Evidence from high-resolution three dimensional seismic data. *Mar. Pet. Geol.* **54** 83-95 (2014).
14. Schofield, N. *et al.* Seismic imaging of 'broken bridges': linking seismic to outcrop-scale investigations of intrusive magma lobes. *J. Geol. Soc.* **169** (4), 421-426 (2012).
15. Thomson, K. Volcanic features of the North Rockall Trough: application of visualisation techniques on 3D seismic reflection data. *BVol.* **67** (2), 116-128 (2005).
16. Jackson, C. A. L. Seismic reflection imaging and controls on the preservation of ancient sill-fed magmatic vents. *J. Geol. Soc.* **169** (5), 503-506 (2012).
17. Tian, W. *et al.* The Tarim picrite-basalt-rhyolite suite, a Permian flood basalt from northwest China with contrasting rhyolites produced by fractional crystallization and anatexis. *CoMP.* **160** (3), 407-425 (2010).
18. Chen, M.-M. *et al.* Peridotite and pyroxenite xenoliths from Tarim, NW China: Evidences for melt depletion and mantle refertilization in the mantle source region of the Tarim flood basalt. *Litho.* **204** 97-111 (2014).
19. Magee, C., Maharaj, S. M., Wrona, T., & Jackson, C. A. L. Controls on the expression of igneous intrusions in seismic reflection data. *Geosphere.* **11** (4), 1024-1041 (2015).
20. Bahorich, M., & Farmer, S. 3-D seismic discontinuity for faults and stratigraphic features: The coherence cube. *The Leading Edge.* **14** (10), 1053-1058 (1995).

